



# Gallium ion irradiation induced compaction and hardening of sputter deposited amorphous carbon thin films

Fritz Lehnert<sup>a,\*</sup>, Tilmann Häupl<sup>b</sup>, Bernd Abel<sup>a,b</sup>, S.G. Mayr<sup>a,c,\*</sup>

<sup>a</sup>Leibniz Institute for Surface Modification, Permoserstraße 15, 04318 Leipzig, Germany

<sup>b</sup>Wilhelm-Ostwald-Institute, Faculty of Chemistry and Mineralogy, University of Leipzig, Linnéstraße 3, 04103 Leipzig, Germany

<sup>c</sup>Division of Surface Physics, Faculty of Physics and Earth Sciences, University of Leipzig, Linnéstraße 5, 04103 Leipzig, Germany

## ARTICLE INFO

### Article history:

Received 15 August 2016

Received in revised form 23 September 2016

Accepted 26 September 2016

Available online 29 September 2016

### Keywords:

Ion irradiation

Amorphous carbon

Compaction

Hardening

## ABSTRACT

We investigate sputter deposited amorphous carbon thin films modified by energetic 30 keV gallium ion irradiation. The samples are characterized combining atomic force microscopy and scanning electron microscopy with Raman spectroscopy measurements. Upon ion irradiation the development of a surface depression is observed, which saturates at a fluence of  $10^{16}$  cm<sup>-2</sup>. In this fluence range a transition in material behavior is observable with different analysis techniques. In addition, a surface smoothing and material hardening was measured. Stress relaxation as well as a transition from a sp<sup>2</sup>-rich towards a sp<sup>3</sup>-rich carbon hybridization are discussed as possible origin.

© 2016 Published by Elsevier Ltd

## 1. Introduction

Ion irradiation is a versatile tool for material modification and is widely used, e.g., within semiconductor industry, because it is able to modify the surface properties with nanometer precision [1]. Moreover, the modification of carbon is interesting as a plethora of applications has its origins in the carbon allotropy. For nanoporous or nanostructured carbon materials membrane and catalyst applications are reported [2–4]. In contrast, hard diamond or diamond like carbon coatings are utilized for wear resistance coatings or imprint lithography mold fabrication [5,6]. Additionally, carbon is interesting for medical application, as it is non-toxic and biocompatible [7,8]. In contrast to purely scientific investigations of ion irradiation effects for MeV ions, ion energies of some keV are technologically highly relevant for surface and interface refining and modification processes [9–11].

Here, we investigated the impact of 30 keV gallium ion irradiation on sputter deposited amorphous carbon thin films, motivated by the potential applications. The effects are mapped and analyzed by atomic force microscopy (AFM), scanning electron microscopy (SEM), AFM-based mechanical property mapping as well as Raman

spectroscopy. In our study we observe a strong material compaction, which is discussed with respect to different models: the forward sputtering mechanism and irradiation induced defect mediated stress relaxation.

## 2. Experimental

Carbon thin films were produced by sputter deposition at high vacuum conditions using wet oxidized silicon wafers with an oxide thickness larger than 700 nm as substrates. The base pressure of the system was  $3 \times 10^{-4}$  or below and the system was flushed with high purity argon at a flow rate of 5 sccm for 5 min prior to sputter deposition. The carbon thin films were then deposited via argon plasma DC magnetron sputtering [12] at an average power of 100 W and an argon flow rate of 15 sccm. The sputtering time was chosen to result in films with a minimum thickness of 300 nm. The subsequent ion irradiation utilized a Carl Zeiss Auriga focused ion beam (FIB) using 30 keV gallium ions from an Orsay Physics COBRA-FIB column and fluences between  $1 \times 10^{14}$  cm<sup>-2</sup> to  $1 \times 10^{18}$  cm<sup>-2</sup> were used for ion irradiation of square areas with length of 10 μm. The samples were aligned for normal ion beam incidence to achieve maximum penetration depth. The ion beam scanned the sample line wise with a pixel dwell time of 0.1 μs and a resolution of 6144 × 4608 pixels, such that the total time of irradiation results in the desired irradiation fluence at the ion currents of 2 pA, 5 pA, 50 pA 600 pA. The

\* Corresponding authors.

E-mail addresses: [fritz.lehnert@iom-leipzig.de](mailto:fritz.lehnert@iom-leipzig.de) (F. Lehnert), [stefan.mayr@iom-leipzig.de](mailto:stefan.mayr@iom-leipzig.de) (S.G. Mayr).

samples were analyzed by atomic force microscopy (AFM) with a Bruker Icon Dimension, by scanning electron microscopy (SEM) with a Carl Zeiss Ultra 55 and by X-ray diffraction (XRD) measurements and X-ray reflectometry (XRR) using a Rigaku Ultima IV and a Seifert XRD 3003 PTS. Both instruments for XRD and XRR measurements use  $\text{CuK}_\alpha$  radiation ( $\lambda = 0,15418$  nm). The sample root mean square (RMS) roughness was determined from AFM images with analysis areas between  $30 \mu\text{m}^2$ . The area varied due to the exclusion of large contamination (e.g. dust particles). For Raman spectroscopy measurements an Olympus IX71 microscope equipped with a Verdi V5 coherent frequency doubled Nd:YAG laser at 532 nm, a HORIBA scientific iHR320 spectrometer and a HORIBA scientific synapse CCD camera were used. The laser output power was set to 500 mW such that after the beam focusing and shaping setup containing optical filters, the sample was measured at  $\approx 5$  mW optical power [13]. With the laser wavelength and the numerical aperture of the objective lens  $\text{NA} = 0.6$  the ideal laser focus diameter is estimated to 440 nm. The elastic properties were determined by AFM in peak force quantitative nanomechanical mapping (PFQNM) mode. That is, because the PFQNM mode of the AFM processes all data on the fly and the measurement software only implements the use for soft materials<sup>1</sup>. The program calculates the modulus using the DMT-model [14] given by the equation

$$F = k_c \delta_c = \frac{4}{3} \left( \frac{1 - \nu_s^2}{E_s} + \frac{1 - \nu_c^2}{E_c} \right)^{-1} \cdot \sqrt{R \cdot \delta_s^3 + F_{adh}} \quad (1)$$

with the force  $F$ , the adhesion force  $F_{adh}$ , the cantilever spring constant  $k$ , the Poisson ratio  $\nu$ , Young's modulus  $E$ , tip radius  $R$ , deformation  $\delta$  and the indices  $c$  and  $s$  denoting the cantilever and sample respectively. However, the implementation for soft materials assumes  $E_c \rightarrow \infty$ , which does not hold for hard materials. Therefore, this was manually corrected for the measurements using a finite  $E_c$  for calculation of the modulus  $E_s$ . The measurement of hard materials requires stiff cantilevers, and thus uncoated silicon cantilevers of type SD-T7L100SPL from NanoWorld AG having a nominal stiffness of  $k_c = 700 \text{ N m}^{-1}$  were chosen. The tip was worn prior to measurement for at least 30 min to reduce tip wear effects during the measurement as demonstrated in previous contact resonance AFM studies [15,16]. In order to determine the tip radius, a reference sample of Si(100) was measured and the equivalent tip radius was calculated to 99 nm. The elastic modulus of 170 GPa for Si(100) was used in all calculations [17]. The errors given for PFQNM measurements are full width at half maximum values of the modulus distribution function. From the physical perspective the measurement is limited by the probe's tip stiffness. For soft samples with  $E_s \ll E_c$  the elastic modulus quantification is directly possible. The elastic modulus of stiffer samples ( $E_s \approx E_c$ ) is usually underestimated and the error increases. For very stiff samples ( $E_s \gg E_c$ ) careful consideration of the measurements is required, however, such stiff materials still yield high elastic moduli allowing for a qualitative assessment on comparative basis within the same measurement.

### 3. Results

The as-deposited carbon thin films exhibit a granular surface structure with typical lateral dimensions below 100 nm observed in SEM analysis and a surface roughness of 2.8 nm as determined by AFM measurements. A density of  $1.6 \text{ g cm}^{-3}$  for the as-deposited film was obtained by XRR measurement, which is low compared to other carbon materials, e.g., graphite with  $2.3 \text{ g cm}^{-3}$  or diamond with

$3.5 \text{ g cm}^{-3}$ , but in good agreement with previous research [18]. The films showed no crystallinity in XRD measurements in the interesting range between  $10^\circ$  to  $60^\circ$  neither in an ordinary  $2\theta/\theta$ -measurement nor in a grazing incidence diffraction scan and are hence considered fully amorphous.

The fluence range for ion irradiation was chosen to be as large as possible. We found that no measurable material change was induced for fluences below  $3 \times 10^{14} \text{ cm}^{-2}$ . On the other hand, the film thickness limits the highest irradiation fluences. For fluences above  $3 \times 10^{17} \text{ cm}^{-2}$  the film was completely sputtered off the silicon substrate. As a consequence the sample treatment and subsequent analysis was limited to the fluence range from  $3 \times 10^{14}$  to  $3 \times 10^{17} \text{ cm}^{-2}$ .

#### 3.1. Surface morphology measurements

After ion irradiation the carbon thin film surface topography was measured by AFM (Fig. 1) and the difference of surface height between irradiated and non-irradiated area is called step height hereafter and displayed in Fig. 2a. The step height was extracted from AFM measurements by the evaluation of the height distribution function. It is clearly visible that a depression of the irradiated areas occurred for all fluences. Moreover the irradiations with different FIB currents align very well, showing that the process is current independent and no effect related to irradiation heating affects the process. Thus, different currents can be applied in order to reach irradiation fluences over three orders of magnitude. In addition to the measurement values (full symbols), a linear dependence as expected for sputtering is displayed (solid line). Comparing the measurements to the aforementioned linear dependence, we assign three different regions: A) a logarithmic decrease of step height below  $10^{16} \text{ cm}^{-2}$ , B) a saturation regime between  $10^{16} \text{ cm}^{-2}$  to  $10^{17} \text{ cm}^{-2}$ , and C) a linear regime above  $10^{17} \text{ cm}^{-2}$ . In combination with the step height evolution we also consider the surface morphology development indicated by the surface RMS roughness given in Fig. 2b. It is apparent that the surface roughness decreased abruptly on the transition from regime A to B with a decrease in RMS roughness by more than 0.5 nm. It is notable that this abrupt transition matches the transition between regimes A and B of the step height measurements (Fig. 2a) and thus clearly indicates that some process affects the surface of the material strongly reaching fluences of  $\sim 10^{16} \text{ cm}^{-2}$ .

The transition in surface morphology was also observed within an analysis of the power spectral density function (PSDF) between regimes A and B. In general, the PSDF was always larger for samples of regime A compared to regime B (Fig. 3). More interesting, for wave numbers  $k > 0.05 \text{ nm}^{-1}$  the samples in regime A show a dependence  $\sim \frac{1}{k^4}$ , but the samples in regime B exhibit a dependence  $\sim \frac{1}{k}$ , that are commonly related to surface diffusion and plastic deformation, respectively [19].

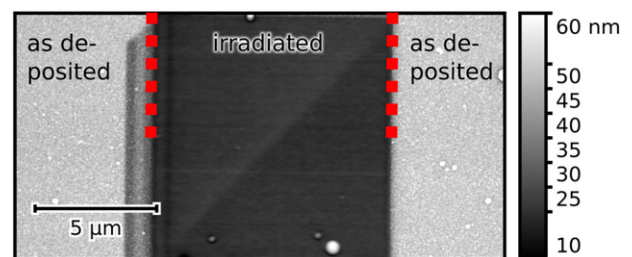


**Fig. 1.** AFM measurement carbon irradiated at a fluence of  $10^{17} \text{ cm}^{-2}$ . The irradiated area is visible in the middle, surrounded by unirradiated material. For the irradiated area a depression is clearly visible and the smoothness can be observed.

<sup>1</sup> While this is not a physical problem itself, it remains difficult in experiments as devices ship with proprietary software with limited configuration options.

Download English Version:

<https://daneshyari.com/en/article/5023927>

Download Persian Version:

<https://daneshyari.com/article/5023927>

[Daneshyari.com](https://daneshyari.com)